 CMES, vol.116, no.2, pp.215-228, 2018

Numerical Analyses of Idealized Total Cavopulmonary Connection Physiologies with Single and Bilateral Superior Vena Cava Assisted by an Axial Blood Pump

Xudong Liu[1], Yunhan Cai[1], Bing Jia[2], Shengzhang Wang[1, *] and Guanghong Ding[1, #]

Abstract: Our study evaluated the hemodynamic performance of an axial flow blood pump surgically implanted in idealized total cavopulmonary connection (TCPC) models. This blood pump was designed to augment pressure from the inferior vena cava (IVC) to the pulmonary circulation. Two Fontan procedures with single and bilateral superior vena cava (SVC) were compared to fit the mechanical supported TCPC physiologies. Computational fluid dynamics (CFD) analyses of two Pump-TCPC models were performed in the analyses. Pressure-flow characteristics, energy efficiency, fluid streamlines, hemolysis and thrombosis analyses were implemented. Numerical simulations indicate that the pump produces pressure generations of 1 mm to 24 mm Hg for rotational speeds ranging from 2000 RPM to 5000 RPM and flow rates of 2 LPM to 4 LPM. Two surgical models incorporated with the pump were found to be insignificant in pressure augmentation and energy boost. The risk assessment of blood trauma and thrombosis generation was evaluated representatively through blood damage index (BDI), particle resident time (PRT) and relative resistant time (RRT). The hemolysis and thrombosis analyses declare the advantage of the pump supported bilateral SVC surgical scheme in balancing flow distribution and reducing the risk of endothelial cell destruction and trauma generation.

Keywords: Computational fluid dynamics, total cavopulmonary connection, bilateral superior vena cava, axial flow blood pump, blood trauma, thrombosis probability.

1 Introduction

Every 2 per 1000 infants are born with the incidence of single ventricular physiology approximately [Pekkan, de Zelicourt, Ge et al. (2005)]. In general, a three stage palliative surgical treatment for single ventricular patients is comprehensively accepted: Norwood, Glenn, and Fontan [Pekkan, Dasi, de Zelicourt et al. (2009)]. As the final step, Fontan procedure has remained optimizing and evolving over the past 30 years [de Zelicourt, Marsden, Fogel et al. (2010)]. The total cavopulmonary connection (TCPC), a surgical approach of the extra-cardiac Fontan, connects the inferior vena cava (IVC) and superior

[1] Institute of Biomechanics, Department of Aeronautics and Astronautics, Fudan University, Shanghai, 200433, China.
[2] Cardiovascular Center, Children's Hospital, Fudan University, Shanghai, 201102, China.
[*] Corresponding Author: Shengzhang Wang. Email: szwang@fudan.edu.cn.
[#] Co-Corresponding Author: Guanghong Ding. Email: ghding@fudan.edu.cn.

vena cava (SVC) to the main pulmonary artery directly. The presence of a single or bilateral SVC is discussed in several studies, where the bilateral SVC has illustrate an advantage in flow distribution to the left pulmonary artery (LPA) and right pulmonary artery (RPA) [Calvaruso, Rubino, Ocello et al. (2008)]. Through this surgery, a univentricular anatomy is created, which leads to an increased workload on the systemic circulation. About 40% Fontan patients developed premature heart failure, with a 5-year mortality rate of 50% [Throckmorton, Lopez-Isaza and Moskowitz (2013)]. Research recommends that the surgical anatomy in conjunction with mechanical support, especially an axial blood pump located in IVC can improve Fontan hemodynamics and patient mortality [Sundareswaran, Pekkan, Dasi et al. (2008)]. To meet these clinical requirements, our group designed a magnetically levitated axial flow blood pump based on the prototypes of systemic VADs from Throckmorton et al. [Throckmorton, Lim, McCulloch et al. (2005)] and the existing product of Jarvik 2000 (Jarvik Heart Inc., New York, NY, USA) to support the TCPC physiology. A protective housing, an inducer, impeller blades, diffuse and straighten region constituted this intravascular axial blood pump. The optimized design aimed at providing a suitable pressure augmentation of blood flow from the IVC to the pulmonary arteries. Simultaneously, the enhanced cardiovascular hemodynamics would be achieved for the improved systemic pressure, increased ventricular filling and augmented cardiac output. The blood pump was expected to serve as a long-term alternative for a bridge to transplant, recovery, and surgical reconstruction.

We constructed a numerical model of the idealized TCPC and incorporated the blood pump into the IVC to evaluate the interactive hemodynamics between the pump and TCPC physiology. The idealized geometry of the TCPC with a 2-diameter offset is provided as the acquirement of the balance between low velocity region and energy efficiency [Marsden, Vignon-Clementel, Chan et al. (2007)]. To verify hemodynamic ascendency of the TCPC physiology supported by the pump with different SVC anatomies, the following two models were analyzed: (i) The pump incorporated an idealized TCPC with a single SVC; (ii) The pump incorporated an idealized TCPC with bilateral SVC (Left SVC and Right SVC).

The CFD analyses included the generation of pressure-flow characteristics, energy assessment, fluid streamlines, hemolysis risk and thrombosis possibility. We also examined hemodynamic performance conditions having pump rotating speeds ranging from 2000 RPM to 6000 RPM, flow rates ranging from 2 L/min to 4 L/min and a uniformed pulmonary arterial pressure depended upon the model under evaluation. This study provides a new phase in the SVC anatomy selection for Fontan physiologies with mechanical supports.

2 Methodology

2.1 Design of the pump

This intravascular axial flow pump is designed for surgical implanting to the IVC. The housing protects the vessel wall from both rotating component and frozen regions. The frozen four blades each of the inducer, diffuser and straightener are separately designed to induce the blood inflow, converse kinetic energy into pressure rise and straighten the outflow. The rotational impeller region with three blades imparts kinetic energy to the

blood. The conceptual design of our axial flow blood pump is exhibited in Fig. 1.

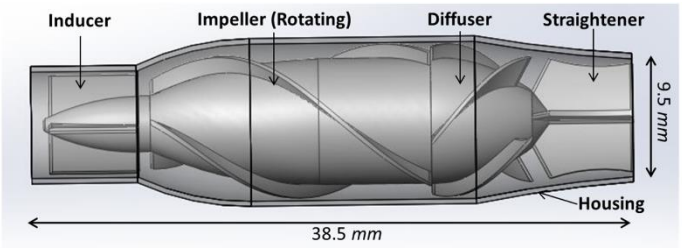

Figure 1: Axial flow blood pump designed for cavopulmonary assistance. This pump consists of a protective housing, an inducer, impeller blades, diffuse and straighten region

2.2 Computational fluid dynamics

We utilized CAD software SolidWorks (SolidWorks Corporation, Concord, MA, USA), to create the pump and idealized TCPC geometries. CFX, the commercial CFD software (ANSYS Incorporated, Canonsburg, PA, USA) is applied to simulate hemodynamic of the TCPC models incorporated with the intravascular blood pump. Fig. 2 illustrates the assembled method of Pump-TCPC considered for this study. The diameters of LPA, RPA and IVC were set 9.5 mm, of which RSVC and LSVC were 8.14 mm and 6.74 mm in the idealized physiologies. ICEM, an ANSYS mesh generation software, was used to build the structure hexahedral grid of the blood pump and the tetrahedral triangular prism element-based mesh for the TCPC analyses. The generation of the 5 layers prism grids has been demonstrated to measure the pressure-flow characteristics at the near-wall regions accurately [de Zelicourt, Marsden, Fogel et al. (2010)]. Tab. 1 describes the computational grid densities of the single pump and the assemblies. For grid quality assurance, the density and convergence of pump and TCPC models were evaluated. A maximal convergence criterion of 1×10^{-4} was applied for each simulation [Bazilevs, Hsu, Benson et al. (2009)].

After the mesh generation, the second-order accurate fluid solver of ANSYS-CFX with Reynolds-Averaged Navier-Stokes (RANS) method followed up in the numerical simulations to solve the equations for the conservation of mass and momentum. The standard k-ε turbulence model has been implemented in these simulations, as which is successfully applicable in a variety of different flow situations, especially in the optimize design of VADs by several researchers [Pekkan, Frakes, de Zelicourt et al. (2005); Throckmorton, Patel-Raman, Fox et al. (2016)].

Table 1: Element counts of the numerical models

Models	Element counts
The axial flow blood pump	1 383 585
Pump, idealized TCPC with a single SVC	2 086 772
Pump, idealized TCPC with bilateral SVC	2 102 815

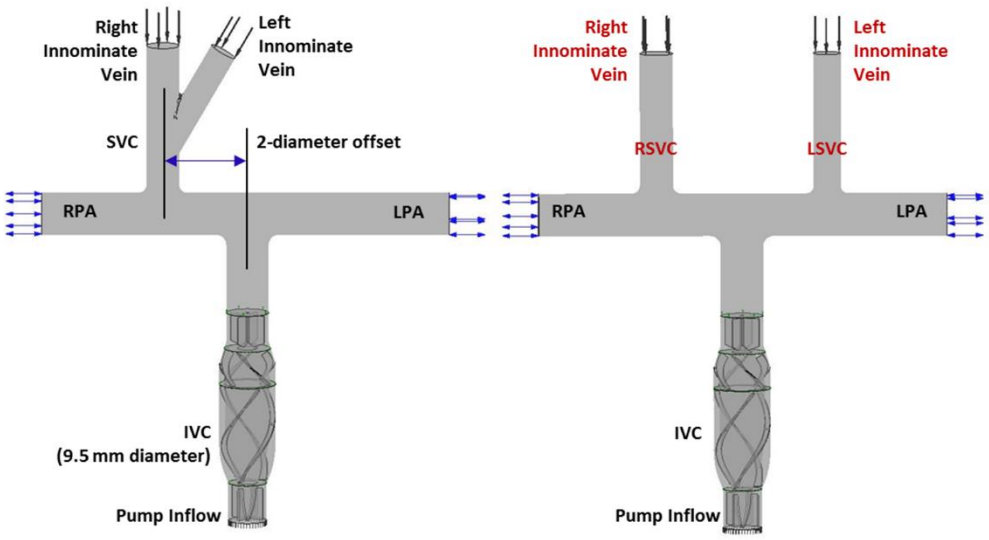

Figure 2: The structure of two TCPC models with single and bilateral SVC incorporated with the blood pump implanted in the inferior vena cava (IVC)

2.3 Boundary conditions

Steady analyses were utilized in the blood flow through the pump and TCPCs with constant boundary conditions for these numerical simulations. To guarantee the fluid velocity values along the TCPC wall would equal zero, the smooth and no-slip boundary condition was assigned. This boundary condition was also applied to the out protective housing of the pump. All the housing and blades of the pump, as well as the vessel walls of TCPC were modeled as rigid. According to the original orientation of the blades, the impeller domain of the pump was designated as a counterclockwise rotating region, while other domains were stationary. The frozen rotor interfaces coupled the impeller domain with other parts through the general grid interface (GGI) method [Riemer, Amir, Reichenbach et al. (2005)]. Five cardiac output (CO) mass inflow rates (2 LPM, 2.5 LPM, 3 LPM, 3.5 LPM, 4 LPM) and five rotating speeds of impeller blades (2000 RPM, 3000 RPM, 4000 RPM, 5000 RPM, 6000 RPM) were specified for each simulation. The inlet flow distribution between SVC and IVC was 45% to 55%, while LSVC and RSVC was 40% to 60%, provided by several studies in Fontan hemodynamics [Soerensen, Pekkan, de Zelicourt et al. (2007)]. The whole blood density, dynamic viscosity and specific heat capacity were set constant as 1060 kg/m^3, 0.0035 Pa·s and 3. 594 kJ/kg/K, respectively [Ou, Huang, Yuen et al. (2016)]. Opening boundary conditions were specified in LPA and RPA to capture any possible irregular flow at the outflow. Considered the pressure augmentation of the pump, the boundary conditions of LPA and RPA, were defined to be a uniformed static pressures to avoid IVC collapse [Throckmorton, Lopez-Isaza, Downs et al. (2013)].

2.4 Energy assessment

The energy boost function of the pump incorporated with TCPC has been estimated by several previous research [Sun, Wan, Liu et al. (2009)]. The energy efficiency of these two Pump-TCPC models with the single or bilateral SVC under different work conditions of the pump was appraised. We calculated the energy gain through the CO ranging from 2 LPM to 4 LPM and the rotating speeds from 2000 RPM to 6000 RPM [Qian, Liu, Itatani et al. (2010)], in accordance with the following equation:

$$E_{gain} = \sum(P_{total\_out})Q_{outlet} - \sum(P_{total\_in})Q_{inlet} \tag{1}$$

Where

$$P_{total} = \bar{P}_{static} + \frac{1}{2}\rho\overline{u_i u_i} \tag{2}$$

In the above equations, ρ is the fluid density, u_i represents the components of the velocity vector, P_{static} corresponds to the static pressure and P_{total} symbolizes the total pressure including both the static pressure and the kinetic energy components, *inlet* and *outlet* represents the entrance and exit surfaces of the Pump-TCPC models, and Q_i is the flow rate of them.

2.5 Hemolysis and Thrombosis Analysis

High rotating speeds of the impeller blades would induce unacceptable shear stress to increase the risk of blood cell damage. Considered the potential of hemolysis and thrombosis, a blood damage analysis was performed in these simulations. Depended on the development path of several blood pumps [Throckmorton, Ballman, Myers et al. (2008)], we choose a dimensionless blood damage index (BDI, *D*), which was widely utilized in the optimizing of pumps, to describe the possibility of blood trauma, according to the equation below:

$$D = \sum_{inlet}^{outlet} 1.8 \times 10^{-6} \cdot \sigma^{1.991} \cdot \Delta t^{0.765} \tag{3}$$

Where Δt corresponds to the stress exposure time, while the scalar stress (σ) is calculated by Bludszuweit's stress formula:

$$\sigma = \left(\frac{1}{6}\sum\left(\sigma_{ii} - \sigma_{jj}\right)^2 + \sum {\sigma_{ij}}^2\right)^{\frac{1}{2}} \tag{4}$$

We tracked the stress history and exposure time of the fluid through particle streamlines in the analyses. A maximum blood damage index of 2% for particle resident time (PRT) of 0.6 s has been accepted as a design criterion along the development of axial flow VADs [Throckmorton, Lopez-Isaza, Moskowitz (2013)].

Another criterion of thrombosis was analyses to the region of TCPC physiology. The relative resident time (RRT) was defined to quantify the state of disturbed flow, as was reasoned by Xiang et al. [Xiang, Natarajan, Tremmel et al. (2011)] relating to the probability of endothelial cell destruction and trauma generation on the vessel wall. The equation followed up:

$$\mathrm{RRT} = \frac{1}{(1-2\times OSI)\times TAWSS} \tag{5}$$

Where

$$\text{TAWSS} = \frac{1}{T} \int_0^T |wss_i| \, dt \tag{6}$$

$$\text{OSI} = \frac{1}{2} \left\{ 1 - \frac{\left| \int_0^T wss_i dt \right|}{\int_0^T |wss_i| dt} \right\} \tag{7}$$

In these three formulas, wss_i corresponds to the instantaneous tangential frictional stress vector of the vessel wall caused by the blood flow and T symbolizes the duration of the rotary cycles. The calculated time-averaged wall shear stress (TAWSS) and oscillatory shear index (OSI), which represented the time integral WSS averaged by the rotary cycles, and the disturbance of it, respectively. We configured 3 transient simulation cases of different rotating speeds (2000 LPM, 4000 LPM and 6000 RPM) for each Pump-TCPC model with the total time of 2 rotary cycles and a time step of 0.25 rotary cycles to calculate the dimensionless RRT.

3 Results

Two independent models were created by assembling the pump to TCPC with single SVC and bilateral SVC. About 50 cases were calculated in these studies with the average Reynolds number of the Pump-TCPC models ranging from 1500 to 4000. Tab. 2 illustrates the pressure augmentation through the pump combined to two TCPC models under two rotating speeds with the inflow rate ranging from 2 L/min to 4 L/min. The deviations of pressure rise between single and bilateral SVC models were not significant, especially for the higher rotational cases. The relationship between inflow rate and pressure augmentation caused by the pump rotary under low or high speeds was revealed in Fig. 3. The axial flow blood pump produced pressure generations of 1 to 36 mm Hg for rotational speeds ranging from 2000 RPM to 6000 RPM under the cardiac output of 2 L/min to 4 L/min. Fig. 3A displays the expected pressure rise across the pump increasing with higher rotational speeds. From this perspective, the impact of flow rate on the pressure rise was not obvious. Fig. 3B was introduced to the influence of flow rate on the pressure rise across the pump, combined with Tab. 2. The increasing cardiac output lead to the decreasing pressure rise at a given rotational speed, as which would theoretically be verified. In accordance with the lump parameter method, the pump, considered as a generator, produced stable power at a fixed rotating speed. Increased flow rate through the pump would inevitably lead to reduced pressure rise.

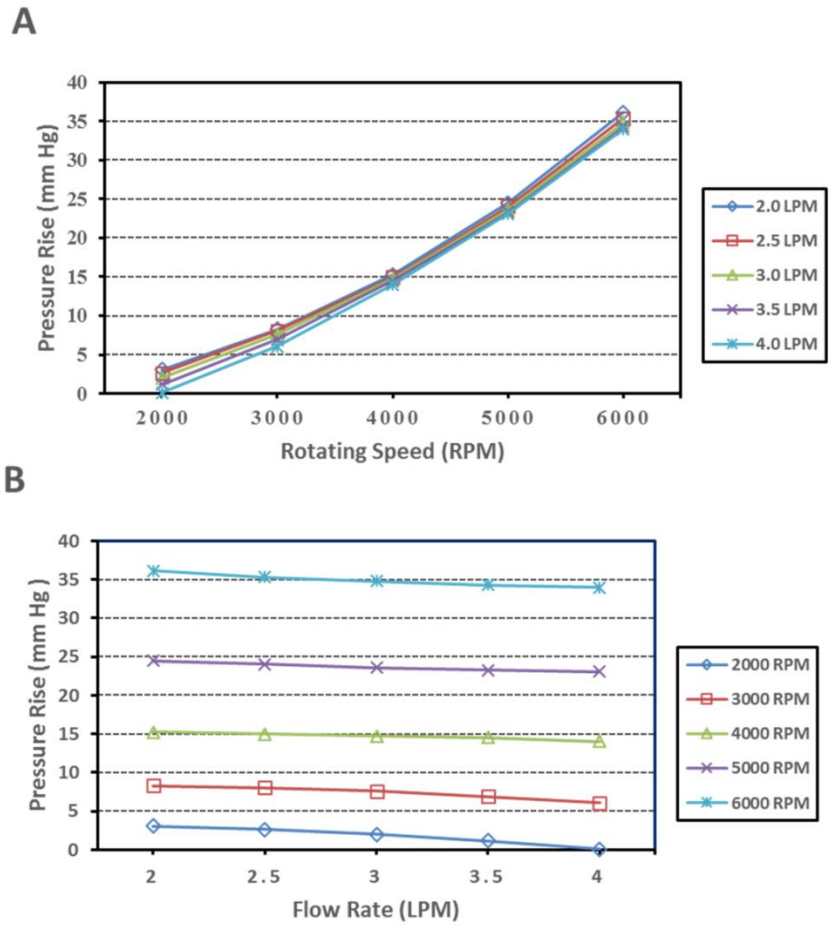

Figure 3: CFD results of the hydraulic characteristics of the blood pump. Flow rates of 2 L/min to 4 L/min were simulated for rotational speeds of 2000 RPM to 6000 RPM. (A) Rotating speed *vs.* pressure rise. (B) Flow rate *vs.* pressure rise

Table 2: Compare of the Pump-TCPC models with single and bilateral SVCs under the rotating speeds of 3000 RPM and 5000 RPM

Cases	3000 RPM						5000 RPM					
	Pressure rise (mm Hg)			Energy gain (m W)			Pressure rise (mm Hg)			Energy gain (m W)		
	Si-SVC	Bi-SVC	Deviation	Si-SVC	Bi-SVC	Deviation	Si-SVC	Bi-SVC	Deviation	Si-SVC	Bi-SVC	Deviation
2.0 LPM	8.29	8.29	0.00%	19.14	19.34	1.06%	24.52	24.52	0.00%	58.68	58.88	0.33%
2.5 LPM	8.08	8.08	0.09%	22.75	23.13	1.68%	24.04	24.04	0.00%	71.46	71.80	0.48%
3.0 LPM	7.58	7.60	0.19%	24.78	25.34	2.28%	23.61	23.61	0.00%	83.52	84.07	0.66%
3.5 LPM	6.93	6.96	0.41%	25.10	25.98	3.48%	23.30	23.30	0.00%	94.87	95.71	0.88%
4.0 LPM	6.06	6.09	0.43%	23.19	24.40	5.25%	23.11	23.11	0.00%	106.30	107.53	1.16%

We also calculated the hydraulic energy of the TCPC with single and bilateral SVC supported by a blood pump in the IVC. Tab. 2 shows the compare in energy gain for the Pump-TCPC models at rotating speeds of 3000 RPM and 5000 RPM. The advantage of bilateral model was more noticeable for increasing inflow rate at lower rotating speed, as the deviation of energy gain enlarged positively. Owing to the resulting superiority of SVC diversion in energy boost, we chose the bilateral model to reveal the interrelation between the flow rate, the rotating speed and the energy boost. Fig. 4 indicates the energy gain of the Pump-TCPC model with bilateral SVC. Generally, the increased energy boost through the whole TCPC region associated with the increasing flow rate at higher rotating speeds. For lower rotating speeds, increasing flow rate enhanced energy gain on lower inflow rate. In contrast, higher inflow rates caused a sharp decrease in the energy improvement of the TCPC physiology.

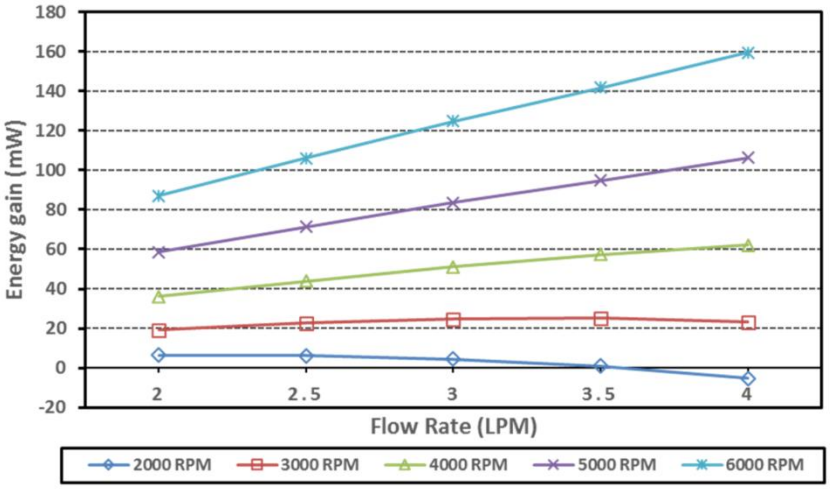

Figure 4: Energy gain due to mechanical assistance of TCPC with bilateral SVC. Flow rates of 2 L/min to 4 L/min were simulated for rotational speeds of 2000 RPM to 6000 RPM

Fig. 5 displays the fluid streamlines in the TCPC with single and bilateral SVC supported by the pump. The results correspond to the operating conditions of cardiac output of 3 LPM and a rotational speed of 4000 RPM. In the single SVC model, stream from SVC was driven directly into the RPA, while about 77 percent of blood flow pumped from IVC shunted to the LPA with a small amount (23%) to the RPA. Conversely, the bilateral model routed stream from LSVC and RSVC to the LPA and RPA, separately. The inferior flow was distributed to the right and left lungs in a suitable proportion (42% *vs.* 58%), consistent with the outcome of traditional Fontan research [Marsden, Vignon-Clementel, Chan et al. (2007)].

Blood damage analyses for each Pump-TCPC model with single or bilateral SVC were implemented under the cardiac output of 3 LPM. Three cases for each model were deployed with the rotating speeds of 2000 RPM, 4000 RPM and 6000 RPM represented to the lower, medium and higher working conditions of the pump, respectively. Tab. 3 lists the compare of the two models in blood trauma risk. The numerical outcomes met the

requirements for avoiding blood damage criterion (BDI<2%, PRT<0.6 s), practically. The single SVC model performed poorly at high rotating speed, as the maximum BDI 1.94% closed to the supreme and maximum PRT 0.66 s exceeded the warning line. Conversely, the bilateral model fulfilled the requirements at a wide range of rotating speeds. In light of the compare above, we released 300 particles at the inferior boundary for each bilateral case.

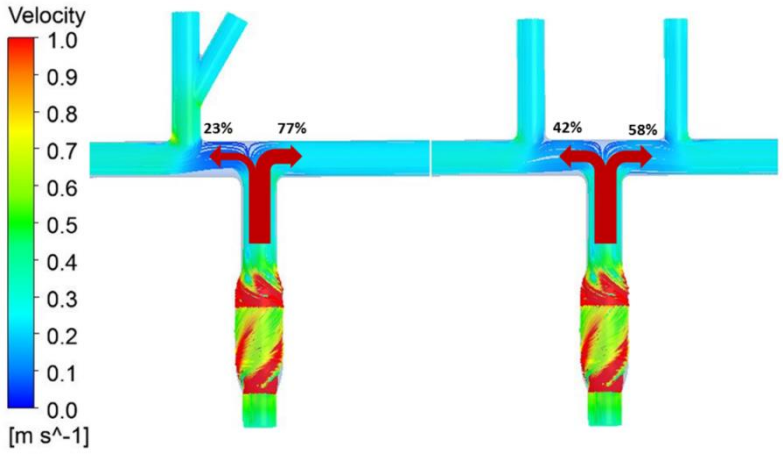

Figure 5: The compare of fluid streamlines in the Pump-TCPC models with single and bilateral SCV, under flow rate of 3 LPM and rotating speed of 4000 RPM

Table 3: Blood damage analyses of two Pump-TCPC models under the cardiac output of 3 LPM

Cases	Main BDI (%)		Maximum BDI(%)		Main PRT (s)		Maximum PRT (s)	
	Si-SVC	Bi-SVC	Si-SVC	Bi-SVC	Si-SVC	Bi-SVC	Si-SVC	Bi-SVC
2000 RPM	0.07	0.07	0.23	0.21	0.25	0.25	0.49	0.51
4000 RPM	0.22	0.22	1.23	1.43	0.16	0.17	0.56	0.43
6000 RPM	0.41	0.40	1.94	1.68	0.13	0.13	0.66	0.48

Fig. 6 combined with the details from Tab. 3, demonstrates the particle distributions of blood damage indices of the bilateral SVC model. Fig. 6A shows a lowest probability of trauma above 3 cases at a rotating speed of 2 000 RPM, as the damage index remains less than 0.12% for 283 particles (94.4%). Fig. 6B illustrates a concentrated distribution on the low value of *D* under the medium rotating speed, while 276 particles (92.0%) have a blood damage index less than 0.4%. Fig. 6C displays that damage index remained a supreme of 0.8% for 280 of 300 particles (93.4%) at a higher rotating speed of the pump.

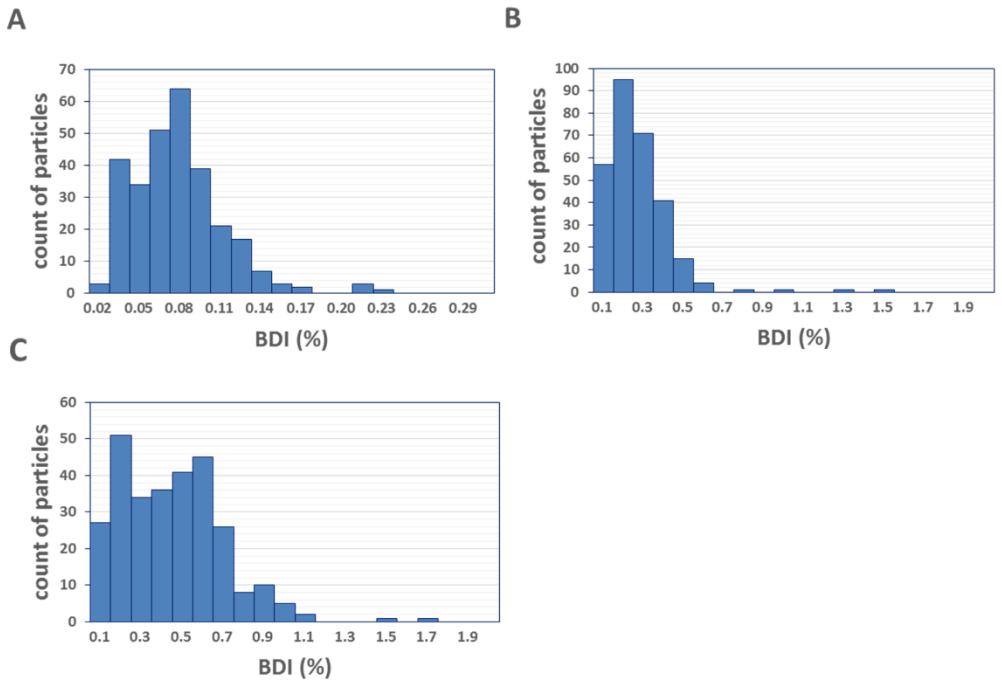

Figure 6: Blood damage indices of the intravascular blood pump for the operating conditions specified in Tab. 2. (A) 2000 RPM. (B) 4000 RPM. (C) 6000 RPM

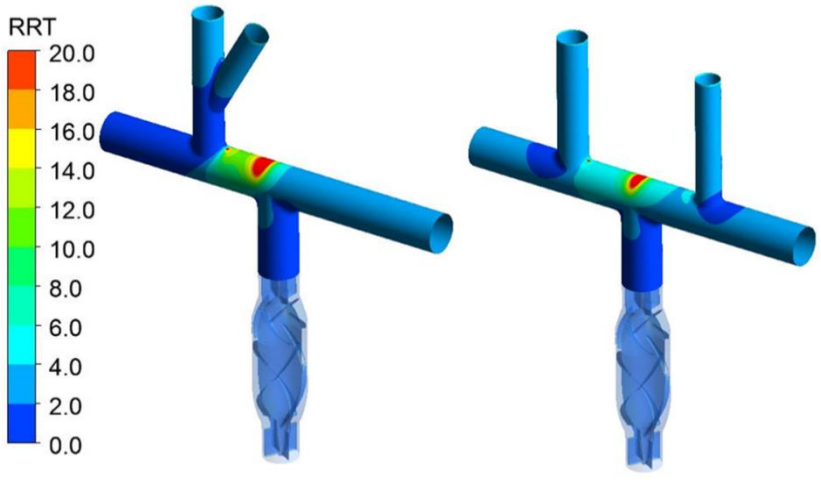

Figure 7: The compare of RRT on the vascular wall for the Pump-TCPC models with single and bilateral SVC, under flow rate of 3 LPM and rotating speed of 4000 RPM

The distribution of RRT on the vessel wall of TCPCs was presented on Fig. 7, intuitively. The high residence time region was observed on the vessel wall opposite directly to the exit of the pump. The size of high RRT region of the bilateral SVC model was much smaller,

when compared to the single one, resulted in a lower risk of endothelial cell destruction and trauma generation.

4 Discussion

Over decades, surgical optimization of the TCPC has been the main issue of researchers and clinicians seeking to minimize energy losses through the vessel configuration (5). The bilateral superior vena cava surgical scheme, which cuts the left innominate vein from the SVC and shunts it to the left pulmonary artery to obtain the persistent left SVC, is reasoned to balance the flow into the pulmonary arteries and then improve the energy efficiency of the TCPC physiology[Tang, Fonte, Chan et al. (2011)]. In recent years, there is a growing interest in the implementation of mechanical assistance in the cavopulmonary simulation to boost pressure and thereby blood flow to the lungs [Throckmorton, Lopez-Isaza, Downs et al. (2013)] The hemodynamic of the TCPC supported by an axial flow blood pump with single and bilateral SVC is numerical simulated to verify the inheritance of the bilateral advantage.

Actually, a pressure augmentation of 2 mm to 6 mm Hg may be sufficient to stabilize and reverse hemodynamic deterioration in Fontan patients [Wang, Pekkan, de Zelicourt et al. (2007)]. This intravascular pump was designed upon the prototypes of VAD. In order to satisfy the hemodynamic requirements of the cavopulmonary circulation, we shrink the sizes of traditional systemic pumps and modify the design parameters, especially for the blades, to receive suitable hydraulic performance from TCPC assistant. As the rotational impeller is the main structure to impart energy to the fluid, this part of traditional blood pumps contains 4 blades to guarantee enough power for systemic circulation. To gain a smaller pressure rise across the pump, we choose a design of 3-blade impeller in this study. Fig. 3 demonstrated that the high rotating speed of the pump generated an excessive pressure rise across the pump, leading to the hypertension of the pulmonary. The pump generated flow rates of 2 L/min to 4 L/min with pressure rises of 1 mm to 24 mm Hg under the rotational speed range from 2000 RPM to 5000 RPM is chosen to consort with the cavopulmonary physiology. According to the energy conversion effect of diffuser, we would further reduce the number of blades, even remove this section from the pump to meet the requirement of a small pressure rise.

To analyze the interactive hemodynamics between the pump and the TCPC, we assess the energy of the total system. Fig. 4 indicated that the incorporation of a blood pump into the IVC resulted in the energy boost at medium and high rotating speeds, while an obvious decrease occurred under the lower speeds as the flow rate upon reaching 4 LPM, especially for the 2000 RPM case. In accordance with previous studies, the increase of energy losses in the TCPC is practically related to higher flow rates [Tang, Fonte, Chan et al. (2011)]. The output of the pump rotating at 2000 RPM could not counteract the energy loss through TCPC physiology under large cardiac outputs. In summary, the rotating speed around 3000 RPM is suitable in pressure augmentation and energy boost for both idealized single and bilateral SVC models.

Blood damage analyses were performed at low, medium and high rotating speeds for each Pump-TCPC model. Fig. 5 and Tab. 2 demonstrated that all cases of bilateral SVC model resulted in a maximum damage index of less than 1.7% and maximum residence time of 0.51 s, indicating a low possibility of blood damage due to interaction with the pump. In

conjunction with surgical optimization of the TCPC, the cavopulmonary assistant may serve as a long-term strategy for Fontan patients. Additional design work will be performed to minimize this flow rotary with a stable performance in hemodynamics.

The compare of single SVC and bilateral SVC model is implemented throughout this simulation. Tab. 2 and Tab. 3 show the similar between these two models in pressure augmentation and energy boost. Though the single model results in an excessive PRT with the BDI closes to supreme of the criterion, the advantage of bilateral model is not entirely significant as expected. To reveal the superiority, the thrombosis analyses represented by RRT are applied. This compare was exhibited in Fig. 7. Combined with the streamlines from Fig. 6, a visible decrease in the region of disturbed flow and more suitable distribution from the inferior were achieved through the bilateral SVC surgery scheme. Vascular patches could be used in this area to enhance the structure, clinically. Above all, the TCPC physiology of bilateral SVC reflects the ascendancy consistently to the previous research of original Fontan optimization, after the incorporation of an axial flow blood pump into the IVC.

This study has several limitations that must be addressed during the next stage of development. The idealized TCPC model could be improved to reflect patient specific geometries. The next step in this analysis is to couple the patient specific models of the TCPC with the blood pump. The superior inlet boundary should be replaced by the opening condition to evaluate and modify possibly existing reverse flow in the SVC due to the implantation of mechanical assistant. Another insufficient place of this study is the blood damage analyses, in which we would take the concentration of variable blood components into consideration during the next study [Karakaya, Baranoglu, Çetin et al. (2015)]. Further, it is much more convictive to take the distribution of the erythrocytes and thrombocytes into the blood trauma analyses through multiphase flow theory and particle transport method [Kim and Kim (2018)]. Hemolysis testing of physical prototypes should be conducted in the future to acquire more realistic confirmation of blood trauma levels for both pump and TCPC region.

5 Conclusions

This study presented hemodynamic numerical simulation of two total cavopulmonary connection surgical schemes incorporated with a blood pump.

1) This magnetically levitated, axial flow blood pump implanted in the IVC is evaluated to generate pressure augmentation and energy boost for patients with failing Fontan physiology.
2) The pump generates flow rates of 2 L/min to 4 L/min with pressure rises of 1 mm to 24 mm Hg under the rotational speed range from 2000 to 5000, will serve as a long-term mechanical assistant with a low risk of blood trauma.
3) A pressure augmentation of as little as 2 mm to 6 mm Hg may be sufficient to stabilize and reverse hemodynamic deterioration in Fontan patients. Our pump can fulfill the requirement under the general work conditions at the rotating speed around 3000 RPM.
4) The bilateral SVC surgical scheme is compared with original single one, resulted in the similar pressure-flow characteristics and energy efficiency.

5) The hemolysis and thrombosis analyses declare the advantage of the pump assisted bilateral SVC surgical scheme in balancing flow distribution and reducing the risk of endothelial cell destruction and trauma generation.

To summarize, the numerical hemodynamic analyses figure out a suitable surgical scheme for the pump implanted Fontan procedure. The bilateral SVC scheme is verified a clear superiority comparing to the single one. Further studies should be implemented in pump modification, patient specific models of TCPC physiology, damage analyses with blood components and experiment design of hemolysis testing.

References

Bazilevs, Y.; Hsu, M. C.; Benson, D. J.; Sankaran, S.; Marsden, A. L. (2009): Computational fluid-structure interaction: methods and application to a total cavopulmonary connection. *Computational Mechanics*, vol. 45, no. 1, pp. 77-89.

Calvaruso, D. F.; Rubino, A.; Ocello, S.; Salviato, N.; Guardi, D. et al. (2008): Bidirectional Glenn and antegrade pulmonary blood flow: Temporary or definitive palliation? *The Annals of Thoracic Surgery*, vol. 85, no. 4, pp. 1389-1395.

de Zelicourt, D. A.; Marsden, A.; Fogel, M. A.; Yoganathan, A. P. (2010): Imaging and patient-specific simulations for the Fontan surgery: Current methodologies and clinical applications. *Progress in Pediatric Cardiology*, vol. 30, no. 1-2, pp. 31-44.

Karakaya, Z.; Baranoglu, B.; Çetin, B.; Yazici, A. (2015): A parallel boundary element formulation for tracking multiple particle trajectories in Stoke's flow for microfluidic applications. *Computer Modeling in Engineering & Science*, vol. 104, no. 3, pp. 227-249.

Kim, K. S.; Kim, M. H. (2018): Simulation of solid particle interactions including segregated lamination by using MPS method. *Computer Modeling in Engineering & Sciences*, vol. 116, no. 1, pp. 11-29.

Marsden, A. L.; Vignon-Clementel, I. E.; Chan, F. P.; Feinstein, J. A.; Taylor, C. A. (2007): Effects of exercise and respiration on hemodynamic efficiency in CFD simulations of the total cavopulmonary connection. *Annals of Biomedical Engineering*, vol. 35, no. 2, pp. 250-263.

Ou, C.; Huang, W.; Yuen, M. M.; Qian, Y. (2016): Hemodynamic modeling of leukocyte and erythrocyte transport and interactions in intracranial aneurysms by a multiphase approach. *Journal of Biomechanics*, vol. 49, no. 14, pp. 3476-3484.

Pekkan, K.; de Zelicourt, D.; Ge, L.; Sotiropoulos, F.; Frakes, D. et al. (2005): Physics-driven CFD modeling of complex anatomical cardiovascular flows? A TCPC case study. *Annals of Biomedical Engineering*, vol. 33, no. 3, pp. 284-300.

Pekkan, K.; Frakes, D.; de Zelicourt, D.; Lucas, C. W.; Parks, W. J. et al. (2005): Coupling pediatric ventricle assist devices to the fontan circulation: Simulations with a lumped-parameter model. *ASAIO Journal*, vol. 51, no. 5, pp. 618-628.

Pekkan, K.; Dasi, L. P.; de Zelicourt, D.; Sundareswaran, K. S.; Fogel, M. A. et al. (2009): Hemodynamic performance of stage-2 univentricular reconstruction: Glenn *vs.* hemi-Fontan templates. *Annals of Biomedical Engineering*, vol. 37, no. 1, pp. 50-63.

Qian, Y.; Liu, J. L.; Itatani, K.; Miyaji, K.; Umezu, M. (2010): Computational

hemodynamic analysis in congenital heart disease: Simulation of the Norwood procedure. *Annals of Biomedical Engineering*, vol. 38, no. 7, pp. 2302-2313.

Riemer, R. K.; Amir, G.; Reichenbach, S. H.; Reinhartz, O. (2005): Mechanical support of total cavopulmonary connection with an axial flow pump. *Journal of Thoracic and Cardiovascular Surgery*, vol. 130, no. 2, pp. 351-354.

Soerensen, D. D.; Pekkan, K.; de Zelicourt, D.; Sharma, S.; Kanter, K. et al. (2007): Introduction of a new optimized total cavopulmonary connection. *Annals of Thoracic Surgery*, vol. 83, no. 6, pp. 2182-2190.

Sun, Q.; Wan, D.; Liu, J.; Liu, Y.; Zhu, M.; Hong, H. et al. (2009): Influence of antegrade pulmonary blood flow on the hemodynamic performance of bidirectional cavopulmonary anastomosis: A numerical study. *Medical Engineering and Physics*, vol. 31, no. 2, pp. 227-233.

Sundareswaran, K. S.; Pekkan, K.; Dasi, L. P.; Whitehead, K.; Sharma, S. et al. (2008): The total cavopulmonary connection resistance: a significant impact on single ventricle hemodynamics at rest and exercise. *American Journal of Physiology-Heart and Circulatory Physiology*, vol. 295, no. 6, pp. 2427-2435.

Tang, B. T.; Fonte, T. A.; Chan, F. P.; Tsao, P. S.; Feinstein, J. A. et al. (2011): Three-dimensional hemodynamics in the human pulmonary arteries under resting and exercise conditions. *Annals of Biomedical Engineering*, vol. 39, no. 1, pp. 347-358.

Throckmorton, A. L.; Lim, D. S.; McCulloch, M. A.; Jiang, W.; Song, X. et al. (2005): Computational design and experimental performance testing of an axial-flow pediatric ventricular assist device. *ASAIO Journal*, vol. 51, no. 5, pp. 629-635.

Throckmorton, A. L.; Ballman, K. K.; Myers, C. D.; Frankel, S. H.; Brown, J. W. et al. (2008): Performance of a 3-bladed propeller pump to provide cavopulmonary assist in the failing Fontan circulation. *Annals of Thoracic Surgery*, vol. 86, no. 4, pp. 1343-1347.

Throckmorton, A. L.; Lopez-Isaza, S.; Downs, E. A.; Chopski, S. G.; Gangemi, J. J. et al. (2013): A viable therapeutic option: Mechanical circulatory support of the failing Fontan physiology. *Pediatr Cardiology*, vol. 34, no. 6, pp. 1357-1365.

Throckmorton, A. L.; Lopez-Isaza, S.; Moskowitz, W. (2013): Dual-pump support in the inferior and superior vena cavae of a patient-specific fontan physiology. *Artifical Organs*, vol. 37, no. 6, pp. 513-522.

Throckmorton, A. L.; Patel-Raman, S. M.; Fox, C. S.; Bass, E. J. (2016): Beyond the VAD: Human factors engineering for mechanically assisted circulation in the 21st century. *Artifical Organs*, vol. 40, no. 6, pp. 539-548.

Wang, C.; Pekkan, K.; de Zelicourt, D.; Horner, M.; Parihar, A. et al. (2007): Progress in the CFD modeling of flow instabilities in anatomical total cavopulmonary connections. *Annals of Biomedical Engineering*, vol. 35, no. 11, pp. 1840-1856.

Xiang, J.; Natarajan, S. K.; Tremmel, M.; Ma, D.; Mocco, J. et al. (2011): Hemodynamic-morphologic discriminants for intracranial aneurysm rupture. *Stroke*, vol. 42, no. 1, pp. 144-152.